

# X-ray Diffraction, Multidimensional NMR Spectroscopy, and MM2\* Calculations on Chiral Allyl Complexes of Palladium(II)

Paul S. Pregosin,\* Heinz Rüegger, and Renzo Salzmann

*Inorganic Chemistry, ETH-Zentrum, CH-8092 Zürich, Switzerland*

Alberto Albinati\* and Francesca Lianza

*Chemical Pharmacy, University of Milan, I-20131 Milan, Italy*

Roland W. Kunz

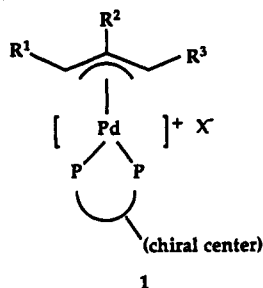
*Organic Chemistry, University of Zürich, CH-8057 Zürich, Switzerland*

Received July 7, 1993\*

The solid-state structure of  $[\text{Pd}(\eta^3\text{-C}_{10}\text{H}_{15})(R\text{-}(+)\text{-BINAP})](\text{CF}_3\text{SO}_3)$ , **3a**, and multidimensional  $^1\text{H}$ ,  $^{13}\text{C}$ , and  $^{31}\text{P}$  NMR spectroscopy and MM2\* calculations for  $[\text{Pd}(\eta^3\text{-C}_{10}\text{H}_{15})(S,S\text{-CHIRAPHOS})](\text{CF}_3\text{SO}_3)$ , **4**, are presented. The various solid- and solution-state structural parameters are compared with literature analogues and differences discussed. Some of the structural distortions observed in both of these  $\eta^3$   $\beta$ -pinene allyl complexes are suggested to arise from electronic effects associated with substituted allyl ligands. The calculations suggest that the chiral array of four phenyl substituents for BINAP is somewhat different from that for CHIRAPHOS, with the phenyl groups for the latter having markedly less "axial" and "equatorial" character. Results from catalytic allylation experiments support the idea of a difference in the chiral array. Crystallographic data for **3a** are as follows: space group  $P6_1$  (No. 169),  $a = 11.787(2)$  Å,  $c = 59.63(1)$  Å,  $V = 7179(2)$  Å<sup>3</sup>,  $Z = 6$ .

## Introduction

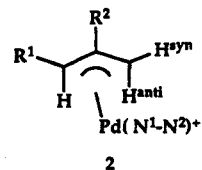
Homogeneous catalytic allylation is a reaction of synthetic interest,<sup>1</sup> and this is especially true if chiral products can be prepared with substantial enantiomeric excesses.<sup>2</sup> For the case where the catalyst is based on a chiral bidentate phosphine complex of palladium(II)<sup>2-6</sup> one can isolate an allylic intermediate related to **1** (there are other



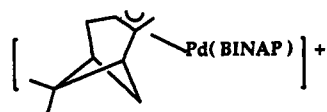
possibilities for **1**, e.g., there can be two R groups on a terminal carbon, the chirality can be on phosphorus as opposed to the carbon backbone, etc.). The mechanism of the allylation reaction is now reasonably well under-

stood,<sup>7</sup> however there are a number of pathways which can lead to reduced optical yields.<sup>4</sup>

We have become interested in both the subtle<sup>8</sup> as well as the gross<sup>9</sup> structural aspects of complexes such as **1**. Specifically, for cationic complexes such as **2** we have



shown<sup>8</sup> that there is a selective rehybridization of the terminal allyl carbons such that the *anti* protons move out of the allyl plane and away from the metal. In addition we have considered the nature of the chiral pocket formed by the diastereomeric  $\beta$ -pinene allyl BINAP complexes, **3**, using 2-D  $^1\text{H}$ -NOESY methods.<sup>9</sup> We have been par-



**3 a = R (+) BINAP**

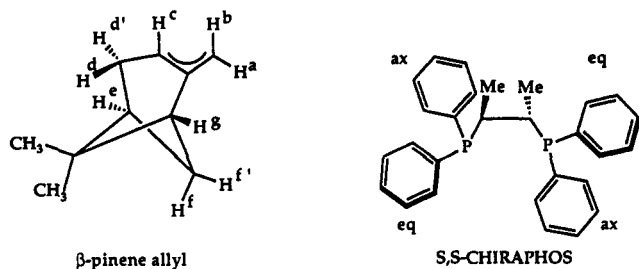
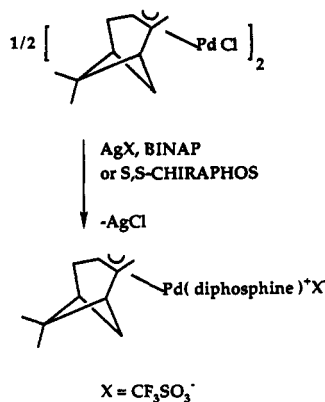
**3 b = S (-) BINAP both as CF<sub>3</sub>SO<sub>3</sub> salts**

ticularly interested in knowing how the chiral array of

\* Abstract published in *Advance ACS Abstracts*, November 15, 1993.  
 (1) Consiglio, G.; Waymouth, R. M. *Chem. Rev.* **1989**, *89*, 257.  
 (2) Consiglio, G.; Indolese, A. *Organometallics* **1991**, *10*, 3425.  
 (3) Yamamoto, K.; Deguchi, R.; Ogimura, Y.; Tsuji, J. *Chem. Lett.* **1984**, 1657.  
 (4) Mackenzie, P. B.; Whelan, J.; Bosnich, B. *J. Am. Chem. Soc.* **1985**, *107*, 2046. Auburn, P. R.; Mackenzie, P. B.; Bosnich, B. *J. Am. Chem. Soc.* **1985**, *107*, 2033.  
 (5) (a) Hayashi, T.; Yamamoto, A. *Tetrahedron Lett.* **1988**, *29*, 669.  
 (b) Hayashi, T.; Yamamoto, A.; Ito, Y.; Nishioka, E.; Miura, H.; Yanagi, K. *J. Am. Chem. Soc.* **1989**, *111*, 6301.  
 (6) Sawamura, M.; Nagata, H.; Sakamoto, H.; Ito, Y. *J. Am. Chem. Soc.* **1992**, *114*, 2586.

(7) Sawamura, M.; Ito, Y. *J. Am. Chem. Soc.* **1992**, *114*, 2586.  
 (8) (a) Albinati, A.; Kunz, R. W.; Ammann, C. J.; Pregosin, P. S. *Organometallics* **1991**, *10*, 1800. (b) Albinati, A.; Ammann, C.; Pregosin, P. S.; Rüegger, H. *Organometallics* **1990**, *9*, 1826.  
 (9) (a) Rüegger, H.; Kunz, R. W.; Ammann, C. J.; Pregosin, P. S. *Magn. Reson. Chem.* **1992**, *29*, 197. (b) Ammann, C. J.; Pregosin, P. S.; Rüegger, H.; Albinati, A.; Lianza, F.; Kunz, R. W. *J. Organomet. Chem.* **1992**, *423*, 415.

Scheme 1



four phenyl groups in a complexed BINAP interacts with a coordinated allyl ligand and have found that the pseudo-equatorial phenyl groups seem to intrude much more than the corresponding pseudo-axial phenyls. Our NOE data when combined with some simple calculations have allowed us to suggest 3-D solution structures for **3a**, **b**. In this work we (1) report on the solid-state structure for **3a** as determined by X-ray diffraction methods, (2) extend our NMR solution structural work to  $[\text{Pd}(\eta^3\text{-C}_{10}\text{H}_{15})(S,S\text{-CHIRAPHOS})](\text{CF}_3\text{SO}_3)$ , **4**, an analogous  $\beta$ -pinene allyl containing 2*S*,3*S*-2,3-bis(diphenylphosphino)butane (*S,S*-CHIRAPHOS), and (3) utilize MM2\* type calculations to explore the electronic and structural sides of this Pd-allyl chemistry.

### Results and Discussion

The preparation of the complexes as well as our numbering system for the  $\beta$ -pinene allyl is shown in Scheme 1.

**X-ray Structure of 3a.** The solution structural analysis of our BINAP complexes using NMR methods has been, to this point, unsupported by a suitable comparison with a solid-state structure; however, we have now determined the solid-state structure for **3a** and show an ORTEP view of this molecule in Figure 1. Table 1 shows a selection of distances and angles for **3a**, and Tables 2 and 3 give crystallographic and positional parameter information, respectively. Our new results are best understood when taken together with our earlier X-ray results<sup>9b</sup> for  $[\text{Pd}(\eta^3\text{-C}_{10}\text{H}_{15})(4,4'\text{-dimethyl-2,2'-bipyridine})](\text{CF}_3\text{SO}_3)$ , **5**, which contains a  $\beta$ -pinene allyl

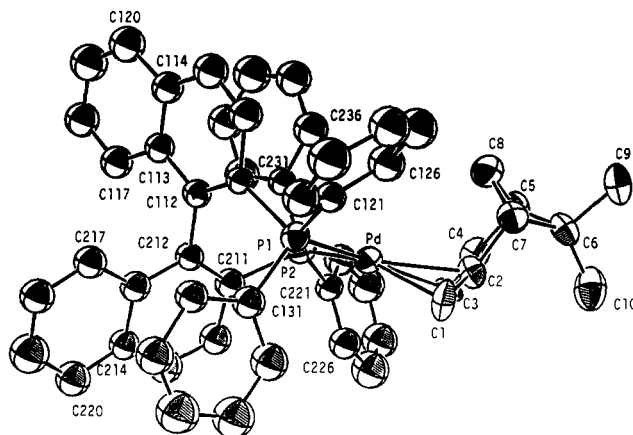
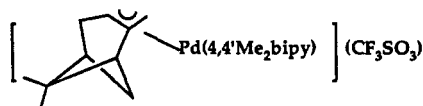


Figure 1. ORTEP plot for the cation of **3a**.

Table 1. Selected Bond Lengths (Å) and Bond Angles (deg) for **3a**

Pd-P(1)	2.312(3)	Pd-P(2)	2.347(5)
Pd-C(1)	2.22(2)	Pd-C(2)	2.26(1)
Pd-C(3)	2.25(1)	C(1)-C(2)	1.45(2)
C(2)-C(3)	1.47(2)	P(1)-C(111)	1.80(1)
P(1)-C(121)	1.81(2)	P(1)-C(131)	1.78(2)
P(2)-C(211)	1.82(1)	P(2)-C(221)	1.81(1)
P(2)-C(231)	1.77(2)		
P(1)-Pd-P(2)	95.8(1)	P(1)-Pd-C(1)	97.8(4)
P(1)-Pd-C(2)	129.1(4)	P(1)-Pd-C(3)	165.4(5)
P(2)-Pd-C(1)	158.8(5)	P(2)-Pd-C(2)	134.6(4)
P(2)-Pd-C(3)	98.1(5)	C(1)-Pd-C(3)	67.6(6)

together with the relatively small nitrogen bidentate. Apart from the usual bond lengths and bond angles, we are specifically interested in comparing **3a** and **5** with respect to (a) the positions of the three allyl carbons relative to a coordination plane defined by the metal and the two coordinated chelate donors, (b) the angle between this latter plane and the plane defined by the allyl carbons, and (c) the locations of distortions in the allyl ligand which arise as a consequence of the differences in steric and electronic properties between the various ligands.

There is no symmetry in **3a**; however, if the allyl is taken as a four-electron donor, then **3a** can be considered as having a local distorted square planar geometry. The Pd-P separations 2.312(3) and 2.347(5) Å are comparable to those found<sup>10</sup> in the allyl complex  $[\text{Pd}(\eta^3\text{-C}(m\text{-xylyl})_2\text{CHCHPh})(S,S\text{-CHIRAPHOS})](\text{BPh}_4)$ , **6**, 2.321(6) and 2.25(1) Å. The three Pd-C(allyl) bond lengths in **3a**, 2.22(2), 2.26(1), and 2.25(1) Å, are longer than the corresponding distances<sup>9b</sup> in **5**, ca. 2.10–2.14 Å, presumably as a consequence of the difference in *trans* influence between a pyridine-type nitrogen and a tertiary phosphine. Interestingly, when compared to the three Pd-C(allyl) bond lengths in **6**, 2.29(2), 2.17(2), and 2.25(2) Å,<sup>10</sup> the three Pd-C(allyl) bond distances in **3a** differ significantly only at the central carbon, which, in **3a**, is further away from the metal. The P-Pd-P chelate angle, 95.8(1)°, is relatively large. The literature<sup>11,12</sup> for coordinated BINAP ligands suggests that ca. 90° would be expected, with the range being ca. 86–93°. The allyl carbon-carbon separations, C(1)-C(2), 1.45(2) Å, and C(2)-C(3), 1.47(2) Å, are as expected relative

(10) Farrar, D. H.; Payne, N. C. *J. Am. Chem. Soc.* 1985, 107, 2054.

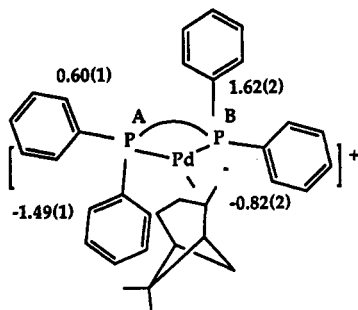
(11) Ashby, M. T.; Khan, M. A.; Halpern, J. *Organometallics* 1991, 10, 2011.

(12) (a) Mashima, K.; Kusano, K.; Ohta, T.; Noyori, R.; Takaya, H. *J. Chem. Soc., Chem. Commun.* 1989, 466. (b) Ohta, T.; Takaya, H.; Noyori, R. *Inorg. Chem.* 1988, 27, 566. (c) Toriumi, K.; Ito, T.; Takaya, H.; Souchi T.; Noyori, R. *Acta Crystallogr.* 1982, B38, 807.



ladium. The analogous angle for **5** is ca. 113°, and for simpler<sup>5,8,9,13</sup> palladium-allyl complexes this angle can be ca. 110–115°.

At this point it is interesting to compare aspects of the X-ray data with our calculated solution structure. The distances of the four *ipso* carbons of the Ph rings with respect to the P–Pd–P plane are shown in the following sketch:



Note that P<sup>A</sup> is *trans* to CH<sub>2</sub> and P<sup>B</sup> is *trans* to CH. The numbers clearly define the pseudo-axial and pseudo-equatorial rings so that one could easily imagine that there would be (and we have found)<sup>7b</sup> selective NOE's from the *ortho* protons of the rings to the three allyl protons. Indeed, if one places the allyl and *ortho* phenyl ring protons in their "ideal" positions, then the X-ray data give the following separations (Å):

	method	
	X-ray	previous calculation <sup>9a</sup>
H <sup>B</sup> <sub>eq</sub> -H <sup>a</sup>	2.88	2.96
H <sup>B</sup> <sub>ax</sub> -H <sup>b</sup>	2.26	2.85
H <sup>A</sup> <sub>eq</sub> -H <sup>c</sup>	2.31	2.56

The previous estimation stems from our calculation.<sup>9a</sup> One must remember that the *anti* protons H<sup>b</sup> and H<sup>c</sup> are known from a neutron diffraction study<sup>15</sup> on Ni( $\eta^3$ -C<sub>3</sub>H<sub>5</sub>)<sub>2</sub> as well as from our earlier X-ray and NMR studies on related complexes<sup>8,9</sup> not to be in their idealized positions as placed in the X-ray estimation. These *anti* protons are bent back out of the allyl plane, away from the metal, by ca. 30° so that the X-ray estimation will be too short. In addition, the observed P–Pd–P angle of ca. 96 is larger than the 92.3° result from the earlier AM1 calculation. This difference will also contribute to the observed discrepancy in the above numbers since opening the angle brings all four Ph groups closer to the allyl ligand. Given these factors, we are pleased that both methods clearly show that the *ortho* protons of the phenyl rings indeed approach the allyl protons in a selective and predictable way.

Before closing this section, we note that, on the basis of the structures for **3a** and **5**, the allyl out-of-plane rotation is electronic in origin but that the opening of the interplane angle (ca. 117° in **3a** vs ca. 113° in **5**) may be due to steric factors.

**NMR Spectroscopy for [Pd( $\eta^3$ -C<sub>10</sub>H<sub>15</sub>)(*S,S*-CHIRAPHOS)](CF<sub>3</sub>SO<sub>3</sub>), **4**.** We have extended our NMR studies to the CHIRAPHOS analogue **4**, and as usual,<sup>9,16,17</sup> we start the NMR analysis with a 2-D <sup>31</sup>P, <sup>1</sup>H-

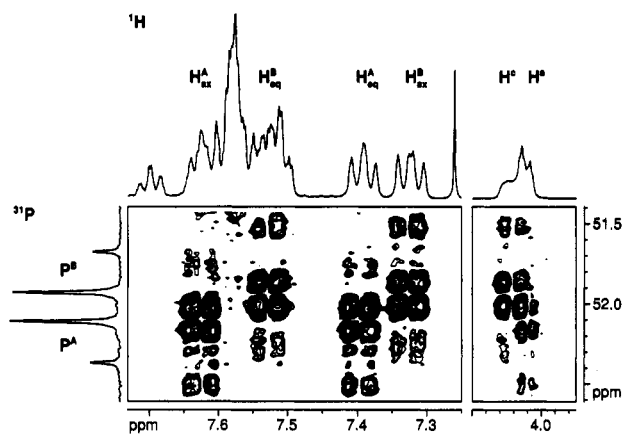


**Figure 2.** Section of the <sup>31</sup>P, <sup>1</sup>H correlation showing the selective correlation of H<sup>A</sup><sub>eq</sub> and H<sup>A</sup><sub>ax</sub> with P<sup>A</sup> and H<sup>B</sup><sub>eq</sub> and H<sup>B</sup><sub>ax</sub> with P<sup>B</sup>, as well as the two correlations from H<sup>c</sup> and H<sup>e</sup> to P<sup>B</sup> and P<sup>A</sup>, respectively.

correlation. Since the *trans* <sup>3</sup>J(P,H) spin-spin couplings are usually larger than the *cis* analogs,<sup>18</sup> a 2-D <sup>31</sup>P, <sup>1</sup>H-correlation accomplishes two goals: (a) the two <sup>31</sup>P spins are assigned (Figure 2 shows two sections of this measurement which demonstrate this point); (b) simultaneously, the *ortho* protons of the four phenyl rings are associated with their corresponding phosphorus resonances. The distinction between the pseudo-axial and pseudo-equatorial phenyl rings can be made by a 2-D <sup>1</sup>H-NOESY measurement, which also allows us to complete all the necessary proton assignments.

Having made these <sup>1</sup>H assignments (which are tabulated in Table 4), we correlated the protons to their corresponding carbons and show these <sup>13</sup>C data in Table 5. This <sup>13</sup>C, <sup>1</sup>H measurement gives us the chemical shifts of the terminal allyl carbons and also reveals that the *ortho* carbon signals of the different axial phenyls are shifted downfield with respect to the corresponding signals from the equatorial phenyls; see Figure 3. This difference may prove to be a useful empirical tool when assigning NMR spectra of CHIRAPHOS complexes. As the electronic effects due to coordination of the two phosphorus donors should be the same for both axial and equatorial phenyls, we presume that this deshielding is a local anisotropic effect. For **4**, the terminal allyl CH and CH<sub>2</sub> signals appear at 80.8 and 67.4 ppm, respectively, whereas these resonances for the *R*-(+) and *S*-(-) BINAP analogues are at 86.4 and 74.5 ppm in **3a** and 79.0 and 72.9 ppm in **3b**, respectively. If one accepts the empiricism<sup>19,20</sup> that changes in the <sup>13</sup>C shift are related to the donor capacity of the *trans* ligand, then it would seem that there are significant differences between these two chelating diphosphines. For the related complex [Pd( $\eta^3$ -C<sub>10</sub>H<sub>15</sub>)(Me<sub>2</sub>PCH<sub>2</sub>-CH<sub>2</sub>PMe<sub>2</sub>)](CF<sub>3</sub>SO<sub>3</sub>),<sup>9b</sup> the terminal allyl carbons appear at 77.4 (CH) and 61.8 ppm (CH<sub>2</sub>), both at rather high field. These <sup>13</sup>C results nicely demonstrate that, even

(16) Albinati, A.; Lianza, F.; Berger, H.; Pregosin, P. S.; Rügger, H.; Kunz, R. W. *Inorg. Chem.* **1993**, *32*, 478.

(17) Leoni, P.; Pasquali, M.; Sommovigo, M.; Laschi, F.; Zanello, P.; Albinati, A.; Lianza, F.; Pregosin, P. S.; Rügger, H. *Organometallics* **1993**, *12*, 1702.

(18) Pregosin, P. S.; Kunz, R. W. *NMR Basic Principles and Progress*; Diehl, D., Fluck, E., Kosfeld, R., Eds.; Springer-Verlag: Berlin, 1979; Vol. 16.

(19) Akermark, B.; Krakenberger, B.; Hansson, S.; Vitagliano, A. *Organometallics* **1987**, *6*, 820.

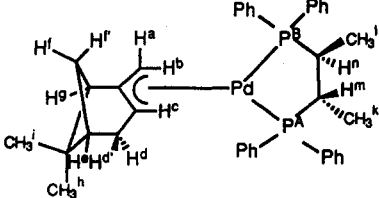
(20) Clark, H. C.; Hampden-Smith, M. J.; Rügger, H. *Organometallics* **1988**, *7*, 2085 and references quoted therein.

(13) Ozawa, F.; Son, T.; Ebina, S.; Osakada, K.; Yamamoto, A. *Organometallics* **1985**, *11*, 171. Hartley, F. R. *The Chemistry of Platinum and Palladium*; Applied Science Publishers: London, 1973; p 430.

(14) Godleski, S. A.; Gundlach, K. B.; Ho, H. Y.; Keinen, E.; Frolow, F. *Organometallics* **1984**, *3*, 21.

(15) Goddard, R.; Kruger, C.; Mark, F.; Stanfield, R.; Zhang, X. *Organometallics* **1985**, *4*, 285.

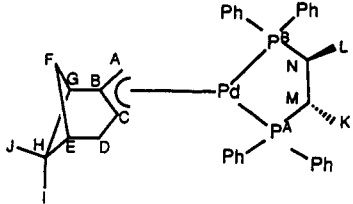
Table 4.  $^1\text{H}$  NMR Data for  $[\text{Pd}(\text{C}_{10}\text{H}_{15})(2\text{S},3\text{S}\text{-CHIRAPHOS})]^+\text{CF}_3\text{SO}_3^-$



	$\delta$	$^nJ(\text{P},\text{H})^b$
a	4.01	7.8
b	2.78	10.6
c	4.03	13.6
d	2.18	
d'	1.53	
e	1.63	
f	2.15	
f'	0.49	
g	2.00	
h	0.96	
i	1.19	
k	1.20	12.0
l	1.11	11.9
m	2.46	
n	2.31	
<i>ortho</i> protons		
$\text{H}_{\text{ax}}^{\text{A}}$	7.62	
$\text{H}_{\text{eq}}^{\text{A}}$	7.37	9.2
$\text{H}_{\text{ax}}^{\text{B}}$	7.30	10.6
$\text{H}_{\text{eq}}^{\text{B}}$	7.50	

<sup>a</sup>  $\delta$  values (in ppm, relative to TMS) have been measured in  $\text{CDCl}_3$  at 297 K and at 500 MHz. <sup>b</sup> Coupling constants in Hz.

Table 5.  $^{13}\text{C}$  and  $^{31}\text{P}$  NMR Data for  $[\text{Pd}(\text{C}_{10}\text{H}_{15})(2\text{S},3\text{S}\text{-CHIRAPHOS})]^+\text{CF}_3\text{SO}_3^-$



	$\delta^a$	$^nJ(\text{P},\text{C})^b$
CA	67.1	29.6 (trans), 6.2 (cis)
CB	145.6	6.5 (trans), 6.5 (cis)
CC	80.7	29.5 (trans), 8.5 (cis)
CD	28.4	
CE	39.1	
CF	29.8	
CG	47.1	
CH	37.9	
CI	21.7	
CJ	25.7	
CK	13.7	14.2 ( $n=3$ ), 3.7 ( $n=2$ )
CL	13.8	14.3 ( $n=3$ ), 3.8 ( $n=2$ )
CM	37.9	28.8 ( $n=1$ ), 18.5 ( $n=2$ )
CN	34.5	28.0 ( $n=1$ ), 17.9 ( $n=2$ )
<i>ortho</i> carbons		
$\text{C}_{\text{ax}}^{\text{A}}$	133.4	13.2
$\text{C}_{\text{eq}}^{\text{A}}$	131.3	12.5
$\text{C}_{\text{ax}}^{\text{B}}$	135.2	13.0
$\text{C}_{\text{eq}}^{\text{B}}$	129.4	
PA	52.2	$^2J(\text{P}^{\text{A}},\text{P}^{\text{B}}) = 51.8$
PB	51.8	$^2J(\text{P}^{\text{A}},\text{P}^{\text{B}}) = 51.8$

<sup>a</sup> Values in ppm, relative to TMS [ $^1\text{H}$ ,  $^{13}\text{C}$ ] and  $\text{H}_3\text{PO}_4$  [ $^{31}\text{P}$ ] for  $\text{CDCl}_3$  solutions at 297 K and at 500 MHz. <sup>b</sup> Coupling constants in Hz.

within a related donor set, the bonding to the allyl carbons can be quite different.

An analysis of the various cross-peaks from the NOESY spectrum reveals several interesting features. One of the two geminal methyl groups (that leaning toward the allyl carbons) shows an NOE to  $\text{H}^c$ ; see Figure 4. This is

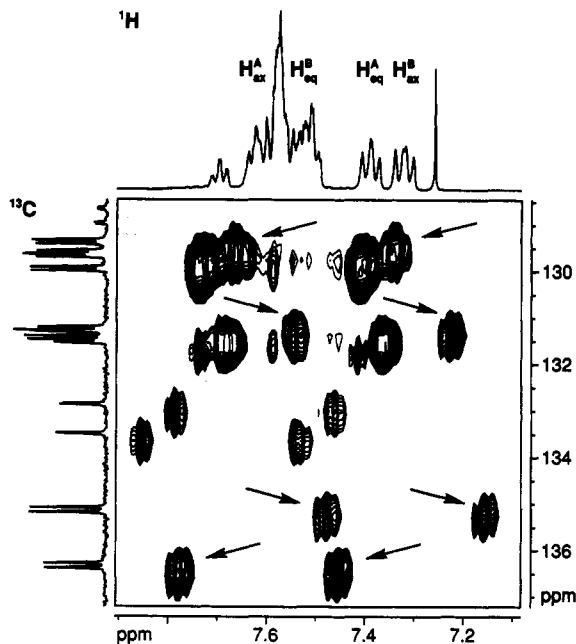


Figure 3. Section of the  $^{13}\text{C},^1\text{H}$  correlation spectrum ( $^1\text{H}$  observation without decoupling of  $^{13}\text{C}$ ) showing the different *ortho* protons ( $\text{H}_{\text{eq}}^{\text{A}}$ ,  $\text{H}_{\text{ax}}^{\text{A}}$ ,  $\text{H}_{\text{eq}}^{\text{B}}$ , and  $\text{H}_{\text{ax}}^{\text{B}}$ ) and their respective carbons. The top four arrows show the C,H cross-peaks to the equatorial carbons, and the bottom four arrows show the cross-peaks to the axial carbons. Note that the axial *ortho* carbons appear at relatively low field.

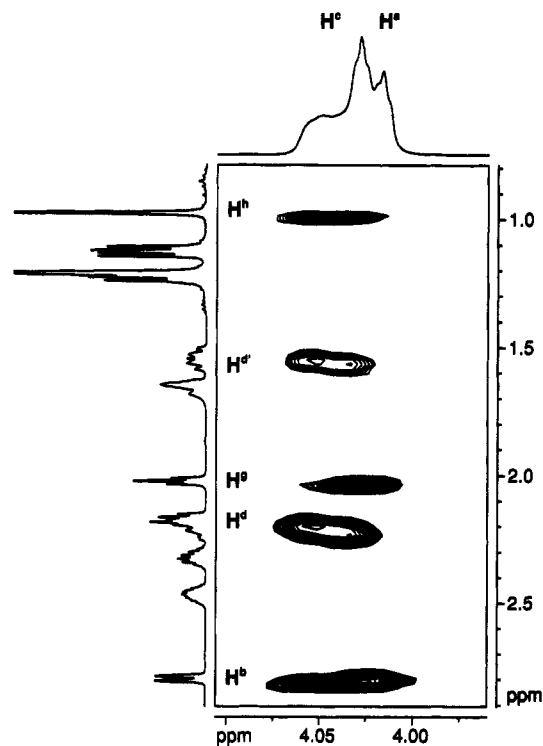
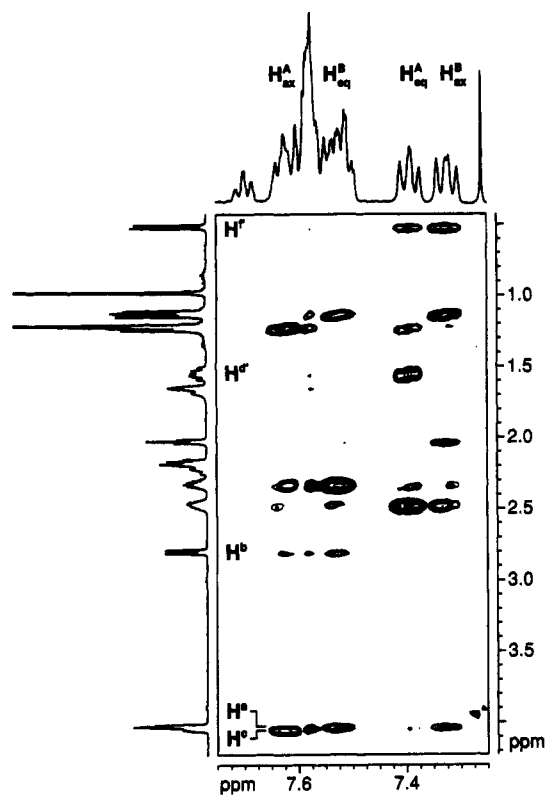


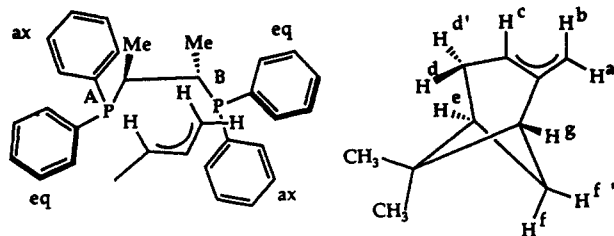
Figure 4. Section of the  $^1\text{H}$  2-D NOESY for 4, with interactions to  $\text{H}^a$  and  $\text{H}^b$ . The cross-peaks (from top to bottom) arise from (a) the allyl proton  $\text{H}^c$  to the pinene methyl  $\text{CH}_3^b$ , (b)  $\text{H}^c$  to  $\text{H}^d$  (and, second from bottom, to  $\text{H}^d$ ), (c)  $\text{H}^a$  to  $\text{H}^g$ , and (d) both  $\text{H}^c$  and  $\text{H}^a$  to  $\text{H}^b$  (500 MHz,  $\text{CDCl}_3$ ).

reasonable if  $\text{H}^c$  is bent back away from the metal, consistent with the proposed selective rehybridization of allyl *anti* C-H bonds. Since  $\text{H}^c$  is bent away from the Pd, the NOE to  $\text{H}^d$  is greater than the NOE to  $\text{H}^d$ . We note that the three  $^1J(^{13}\text{C},^1\text{H})$  values for the allyl protons are 167, 158, and 162 Hz, for  $\text{H}^a$ ,  $\text{H}^b$ , and  $\text{H}^c$ , respectively, with



**Figure 5.** Section of the  $^1\text{H}$  2-D NOESY for 4, with interactions to the various *ortho* protons of the P-Ph rings from the allyl (and other) protons (500 MHz,  $\text{CDCl}_3$ ).

the *syn* proton value clearly larger than those for the *anti* protons. The *syn* proton  $\text{H}^a$  shows a strong NOE to the *ortho* ring protons of  $\text{P}^{\text{B}}_{\text{eq}}$  but only a modest NOE to the *ortho* ring protons of  $\text{P}^{\text{B}}_{\text{ax}}$ . Moreover, the *anti* proton  $\text{H}^b$  shows a moderate NOE to  $\text{P}^{\text{B}}_{\text{eq}}$  and a weak NOE to the *ortho* ring protons of  $\text{P}^{\text{A}}_{\text{ax}}$  (see Figure 5). These observations would be consistent with an anticlockwise out-of-plane rotation of the allyl, as shown in the following sketch (with the Pd and the remaining allyl ligand atoms omitted for clarity):



However, this rotation is not supported by our calculations (*vide infra*). There is also a strong NOE from the *ortho* phenyl protons of  $\text{P}^{\text{A}}_{\text{eq}}$  to  $\text{H}^d$ .

Both the *ortho* ring protons of  $\text{P}^{\text{A}}_{\text{eq}}$  and  $\text{P}^{\text{B}}_{\text{ax}}$  show strong NOE's to  $\text{H}^f$  but no NOE to  $\text{H}^e$ . These two strong NOE's are not expected if the phenyl groups take up static pseudo-axial and pseudoequatorial positions. For the complex  $[\text{Pd}(\eta^3\text{-C}_{10}\text{H}_{15})(\text{S-BINAP})](\text{CF}_3\text{SO}_3)$  there is only one strong NOE from  $\text{H}^{\text{B}}_{\text{ax}}$  to  $\text{H}^f$  suggesting that the array of phenyl groups is different for these two complexes (although they possess the same allyl). In addition, the chemical shift of  $\text{H}^f$  in the CHIRAPHOS analogue at  $\delta = 0.46$  is at much lower frequency (higher field) than that found for  $\text{H}^f$  in  $[\text{Pd}(\eta^3\text{-C}_{10}\text{H}_{15})(\text{S-BINAP})](\text{CF}_3\text{SO}_3)$ ,  $\delta = 1.20$  (the analogous *R*-(+)-BINAP complex has  $\text{H}^f$  at 1.66

ppm). This shielding is most likely anisotropic in nature and presumably stems from the close proximity of two phenyl rings to  $\text{H}^f$ . The fact that both  $\text{P}^{\text{A}}_{\text{eq}}$  and  $\text{P}^{\text{B}}_{\text{ax}}$  show strong NOE's to  $\text{H}^f$  speaks *against* a large rotation of the allyl ligand, since rotation would move  $\text{H}^f$  much closer to one ring than to the other. We shall return to this point and the question of the chiral array in the discussion on the calculations. A direct comparison of cross-peaks for  $[\text{Pd}(\eta^3\text{-C}_{10}\text{H}_{15})(\text{S-BINAP})](\text{CF}_3\text{SO}_3)$  and 4 is not reliable. However, there are some marked differences; e.g. for  $\text{H}^b$  there is a strong interaction to  $\text{P}^{\text{B}}_{\text{eq}}$  in  $[\text{Pd}(\eta^3\text{-C}_{10}\text{H}_{15})(\text{S-BINAP})](\text{CF}_3\text{SO}_3)$  but a modest to weak interaction with the analogous proton in 4.

In summary, we find the same type of *anti* proton rehybridization in our CHIRAPHOS complex as found in other  $\eta^3\text{-C}_{10}\text{H}_{15}$  complexes, supporting the contention that these are electronic effects associated with the bonding of the  $\beta$ -pinene allyl ligand to Pd(II). There are important differences between 3a and 4, e.g. to  $\text{H}^b$  and  $\text{H}^f$ , suggesting a different chiral array of the phenyl groups. There are hints that the terminal allyl carbons do not lie in the P-Pd-P plane, but the twist may be minimal.

**Calculations.** In order to refine our understanding of the allyl ligand, we have carried out some semi-empirical calculations (AM1 level) on three free allyl ligands. Table 6 shows calculated C-C separations for these model anionic ligands, and we note that there is a tendency for the more highly substituted C-C bond to be longer. Introduction of a positive charge ca. 2.4 Å from the three allyl carbons (changing from model "c" to model "d") does not change the trend but lengthens both bonds slightly. These results are in agreement with the crystallographic data, mentioned above, and suggest an electronic (as opposed to a steric) effect to be responsible for these bond length variations.

We have also carried out calculations for our complexes based on MM2\*<sup>21</sup> with the goal of predicting the solution structure for 4; however, before discussing the lowest energy structure for 4, we comment on a "calibration". We have calculated the structures for the known cationic complexes 7,<sup>14</sup>  $[\text{Pd}(\eta^3\text{-C}_3\text{H}_5)(\text{PMe}_3)_2]^+$ ,<sup>22</sup> and  $[\text{Pd}(\eta^3\text{-C}_3\text{H}_5)(\text{Biphenyl})]^+$ <sup>23</sup> using literature bond lengths and angles as input for MM2\*. Comparison<sup>24a</sup> with their known solid-state structures gives good agreement, with the small differences arising primarily from rotations of the P-Ph groups about the P-C(ipso) bond. In the supplementary material we give a list of calculated and observed bond lengths and bond angles for these complexes. Consequently, we are optimistic that our calculations will qualitatively reflect the molecular structure. Indeed, in Figure 6, we show our most recent calculated structure for 3a (with input data from our new structure) superimposed on its solid-state structure and find relatively good agreement between the two. The differences arise primarily from rotations about the P-C(ipso) carbons; however, *in solution*, we know that there is free rotation about these P-C bonds, so that neither of these two can

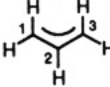
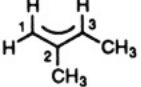
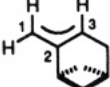
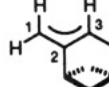
(21) MM2\* is the implementation of Macromodel: Mohamadi, F.; Richards, N. G. J.; Guida, W. C.; Liskamp, R.; Canfield, C.; Chang, G.; Hendrikson, T.; Still, W. C. *J. Comp. Sci.* 1990, 11, 440.

(22) Ozawa, F.; Son, T.; Ebina, S.; Osakada, K.; Yamamoto, A. *Organometallics* 1992, 11, 171.

(23) Knieringer, A.; Scholzer, P. *Helv. Chim. Acta* 1992, 75, 1211.

(24) (a) This process is best carried out on a relatively large computer screen where the two structures (X-ray and calculated) can be superimposed, thereby highlighting differences. (b) As with our results for 4, the calculated structure is consistent with what one finds on the basis of a Cambridge Database search.

Table 6. Distances for Model Anionic Allyl Ligands<sup>a</sup>

	anion			
				
$d(1,2)$	1.370	1.374	1.366	1.383
$d(2,3)$	1.370	1.386	1.394	1.489

<sup>a</sup> Distances are in Å. Allyl anion d is the same as c except that a single positive charge has been introduced ca. 2.4 Å from C(1)–C(3) to polarize the system. The calculations reveal ca. 0.6 units of negative charge on each of the terminal allyl carbons and a small positive charge (ca. 0.04–0.10 units) on the central allyl carbon.

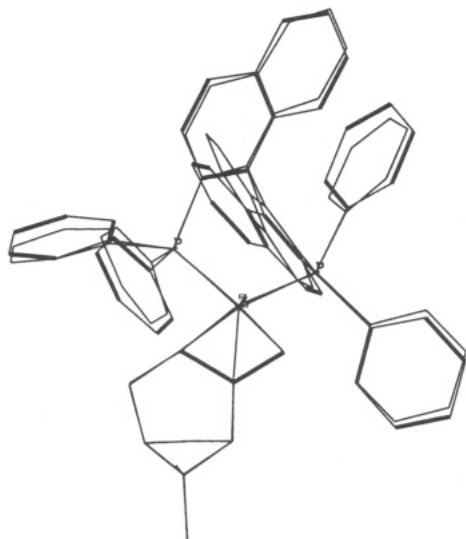


Figure 6. Comparison of the calculated (with bold lines) and experimental solid-state structures for the cation of 3a.

be exactly correct. The calculated structure represents a snapshot, and the X-ray result reflects the packing forces. The structure for 3a shows marked equatorial and axial character for the P–Ph rings.<sup>24b</sup>

Calculations for 4 reveal five different conformations with relatively similar energies, and we show the lowest energy structure in Figure 7. All five structures differ, once again, primarily in the extent to which the Ph groups are rotated about the P–C(ips) bonds. All of these have the two terminal allyl carbons roughly in the P–Pd–P plane, and all of these clearly show that there are *no* marked axial or equatorial phenyl substituents. This result is in agreement with what one would expect for five-membered chelate rings of the CHIRAPHOS type, i.e., with a P–M–P–C(sp<sup>3</sup>)–C(sp<sup>3</sup>) ring, based on a Cambridge Database search. Specifically, the placement of the phenyl substituents is very similar to what has been observed<sup>25</sup> and calculated<sup>26</sup> in some rhodium(I) complexes of CHIRAPHOS. Given that the various structures are all within ca. 3 kcal in energy, it seems presumptuous to speak of a single solution structure. Analysis of the various interligand proton separations reveals the following: (a) There are sufficiently close contacts in the two lowest energy structures (which are ca. 1.5 kcal apart in energy) to explain all of the observed strong NOE's. (b) H<sup>b</sup> is never close to P<sup>B</sup><sub>ax</sub> and can approach P<sup>A</sup><sub>ax</sub> to within ca. 3.5 Å, so that a modest NOE is reasonable. Consequently, a structure with the terminal allyl carbons in the coordination plane can

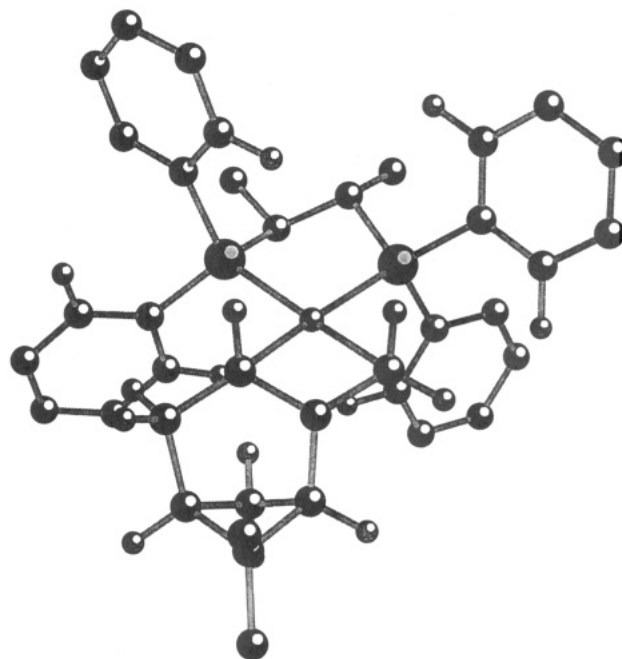


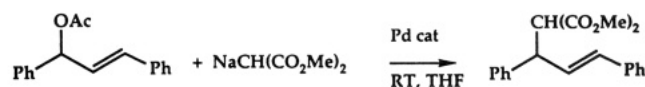
Figure 7. Calculated lowest energy structure for the cation of 4.

be considered as being consistent with the NOE data. (c) H<sup>c</sup> is ca. 2.9 Å from the proximate CH<sub>3</sub><sup>h</sup> group and is bent away from the allyl plane (the calculation suggests ca. 27° in the BINAP complex). (d) H<sup>g</sup> is ca. 3.1 Å from P<sup>B</sup><sub>ax</sub>, and we do observe a medium-strength NOE cross-peak for these two spins.

A comparison of the calculated BINAP and CHIRAPHOS structures, in our Pd(II) complexes, suggests that the phosphorus phenyl groups of the former bidentate ligand intrude more into the sphere of the allyl ligand than do those of the latter ligand.

In conclusion, our calculations clearly show differences between the chiral arrays for our BINAP and CHIRAPHOS complexes and that these differences are supported by the NMR spectroscopy. For 4 it is difficult to speak of a single structure, but since the NMR reveals that P–C(ips) rotation is free, this is an expected result.

**Catalytic Allylation.** Given that we find different chiral arrays for CHIRAPHOS and BINAP in our Pd(II) complexes, we have considered the catalytic allylation shown below:



For this reaction Auburn et al.<sup>4b</sup> have reported an enantiomeric excess of 22% starting from a preformed

(25) Ball, R. G.; Payne, N. C. *Inorg. Chem.* 1977, 16, 1137.

(26) Giovanetti, J. S.; Kelly, C. M.; Landis, C. R. *J. Am. Chem. Soc.* 1993, 115, 4040.

CHIRAPHOS allyl precursor. We have carried out the same reaction, in  $\text{CH}_2\text{Cl}_2$ , using the Pd(0) complex  $\text{Pd}_2$ -(dibenzylidene acetone)<sub>3</sub> and *S*-(-)-BINAP and find an enantiomeric excess of ca. 90%, as determined by HPLC with a chiral column (see Experimental Section). At this point one should not overinterpret this result. However, since we find a more pronounced axial, equatorial array for BINAP than for CHIRAPHOS and we know there is a larger P-Pd-P angle (ca 96°) in the BINAP complex **3a** relative to what one finds for the five-membered ring of CHIRAPHOS, ca. 86°,<sup>10</sup> it is reasonable to believe that the phenyl rings in the BINAP analogue will be pushed forward toward the allyl, producing a more crowded and perhaps more selective chiral pocket. We do not have enough examples to generalize but are encouraged to think that our structural results are reflected in the catalytic chemistry.

### Experimental Section

The ligands *S,S*-CHIRAPHOS and *S*-BINAP were commercially available. Complex **3a** was prepared by us, previously.<sup>2b</sup> The chloro-bridged dimer was prepared according to the literature.<sup>27</sup> The NMR spectra were obtained from  $\text{CDCl}_3$  solutions using a Bruker AMX 500 spectrometer. Standard pulse sequences were used for the NOESY,<sup>28</sup> <sup>13</sup>C,<sup>1</sup>H,<sup>29</sup> and <sup>31</sup>P,<sup>1</sup>H<sup>30</sup> spectra. NOESY spectra were measured using 0.8- and 1.0-s mixing times.

**Crystallography.** Crystals of the BINAP complex suitable for X-ray diffraction were obtained from a  $\text{CHCl}_3$ /hexane/ether (3:3:1) solution and are air stable. However, these crystals, obtained with great difficulty, were all twinned; nonetheless it was eventually possible to find a crystal (fwhm of peaks in the range 0.87–0.93° for 4.0 <  $\theta$  < 19.0°) in which the angular separation of the peaks belonging to the two individuals was wide enough to allow the indexing and the collection of the intensities of only one of the two.

An Enraf-Nonius CAD4 diffractometer was used for the screening of the crystals, for the unit cell and space group determination, and for the data collection. Unit cell dimensions were obtained by least squares fit of the  $2\theta$  values of 25 high-order reflections (9.2 <  $\theta$  < 19.0°) using the CAD4 centering routines. Selected crystallographic and other relevant data are listed in Table II.

Data were measured with variable scan speed to ensure constant statistical precision on the collected intensities. Three standard reflections were used to check the stability of the crystal and of the experimental conditions and measured every 1 h; no significant variation was detected. The orientation of the crystal was checked by measuring three other reflections every 300 measurements.

A total of 12 130 reflections (in the quadrant  $\pm h, +k, +l$ ) were collected and after correction for Lorentz and polarization factors, using the data reduction programs of the MOLEN crystallographic package,<sup>31</sup> were averaged. A set of 250 reflections, equivalent by symmetry, but differing by more than  $5\sigma(I)$  were rejected as possibly affected by the second individual of the twin, thus leaving a set of 4207 independent reflections that were used in the solution and refinement of the structure. The data were corrected empirically for absorption using the program DIFABS at a later stage.<sup>32</sup> The standard deviations on intensities were calculated in term of statistics alone, while those on  $F_o$  were calculated as reported in Table 2. The structure was solved by

a combination of direct and Fourier methods and refined by full-matrix least squares. The function minimized was  $[\sum w(|F_o| - 1/k|F_c|)^2]$  with  $w = [(F_o)]^{-1}$ . No extinction correction was deemed necessary.

The scattering factors used, corrected for the real and imaginary parts of the anomalous dispersion, were taken from the literature.<sup>33</sup> Anisotropic temperature factors were used for the palladium, phosphorus, and the carbon atoms of the  $\beta$ -pinene ligand; all the others were treated isotropically. The triflate counterion is, as often found, disordered; it proved impossible to construct a model for this disorder, and only the strongest peaks in the Fourier difference maps, corresponding to one possible orientation, were retained and refined leading only to an approximate geometry.

The contribution of the hydrogen atoms in their idealized positions (C-H = 0.95 Å, B = 5.0 Å<sup>2</sup>) was taken into account but not refined. Upon convergence (no parameter shift > 0.2 $\sigma(p)$ ) the final Fourier difference map showed only significant peaks (< 0.7 e Å<sup>-3</sup>) around the disordered counterion. All calculations were carried out by using the Enraf-Nonius MOLEN crystallographic programs.<sup>31</sup> The handedness of the crystal was tested by refining the two enantiomorphs. The positional parameters of the enantiomer giving the lower  $R_w$  factor<sup>34</sup> are listed in Table 3.

**Preparation.**  $[\text{Pd}(\eta^3\text{-C}_{10}\text{H}_{15})(\text{S,S-CHIRAPHOS})](\text{CF}_3\text{SO}_3)$ , **4**, was prepared via addition of the chiral phosphine (22.7 mg, 0.053 mmol) to a solution of the chloro-bridged dimer (14.5 mg, 0.036 mmol) in 5 mL of methanol. Stirring for 10 min to afford a clear yellow solution was followed by addition of  $\text{Ag}(\text{CF}_3\text{SO}_3)$  (16.5 mg, 0.056 mmol). The precipitate which results was filtered through Celite and the filtrate concentrated. Dissolving in a minimum amount of  $\text{CHCl}_3$  and covering with a ca. 10-fold excess of ether gives a crystalline product which can be washed with cold ether to afford 15.7 mg (53%) of **4**. Anal. Calc for  $\text{C}_{39}\text{H}_{43}\text{F}_3\text{O}_3\text{P}_2\text{PdS}$  (817.18): C, 57.32; H, 5.30. Found: C, 56.95; H, 5.76.

The catalytic experiment with *S*-BINAP was carried out as described by von Matt et al.<sup>35</sup>

Calculations were carried out using MM2\*, the MM2 implementation of the MacroModel V3.0. The parameters not available were optimized using data from the literature and specifically from the Cambridge database (CEKKOS, JOLZT, JUBVUX) together with data from our structure of **3a**. The resulting agreement between calculated and experimental structures is good (bond length < 0.05 Å, mean bond angles < 1°). Parameters are available as supplementary material upon request. For the CHIRAPHOS complex, a conformational analysis including both rotation of the phenyl rings and chelate conformation was carried out, with 15 different conformations, all within 7 kcal, found. The five energetically most favored structures have both chelate methyl groups in equatorial positions (in keeping with the observed <sup>3</sup>J(P,CH<sub>3</sub>) coupling constants, ca. 14 Hz, shown in Table 5). These five structures differ mainly in the arrangement of the phenyl groups.

**Acknowledgment.** A.A. thanks the CNR for a grant. P.S.P. thanks the Swiss National Science Foundation as well as the ETH for support and the Johnson-Matthey Research Foundation, Reading, England, for the loan of precious metals.

**Supplementary Material Available:** Tables of calculated positional parameters for the hydrogen atoms, anisotropic displacement parameters, complete bond lengths and bond angles, torsion angles, and selected experimental and calculated distances and angles for **3a** and other structures (15 pages). Ordering information is given on any current masthead page.

OM930460J

(33) *International Tables for X-ray Crystallography*; Kynoch Press: Birmingham, England, 1974; Vol. IV.

(34) Hamilton, W. C. *Acta Crystallogr.* 1965, 13, 502.

(35) von Matt, P.; Pfaltz, A. *Angew. Chem., Int. Ed. Engl.* 1993, 32, 566.

(27) Trost, B. M.; Strege, P. E. *J. Am. Chem. Soc.* 1975, 97, 2534.

(28) Jeener, J.; Meier, B. H.; Bachmann, P.; Ernst, R. R. *J. Chem. Phys.* 1979, 71, 4545.

(29) Summers, M. F.; Marzilli, L. G.; Bax, A. *J. Am. Chem. Soc.* 1986, 108, 4285.

(30) Sklener, V.; Miyashiro, H.; Zon, G.; Miles, H. T.; Bax, A. *FEBS Lett.* 1986, 205, 94.

(31) MOLEN: Molecular Structure Solution Procedure. Enraf Nonius, Delft, The Netherlands, 1990.

(32) Walker, N.; Stuart, D. *Acta Crystallogr., Sect. A* 1983, 39, 159.